Invited Paper

Quantum Well Intermixing : Materials Modeling and Device Physics

E. Herbert Li †
Division of Applied Sciences, Harvard University
Cambridge, MA 02138

ABSTRACT

Quantum well composition intermixing is a thermal induced interdiffusion of the constituent atoms through the hetero-interface. The intermixed structures created by both impurity induced and impurity free or vacancy promoted processes have recently attracted high attention. The interdiffusion mechanism is no longer confined to a single phase diffusion for two constituent atoms, but it can now consist of two or multiple phases and/or for multiple species, such as three cations interdiffusion and two pairs of cation-anion interdiffusion. A review on the impact of intermixing on device physics is presented with many interesting features. For instance, both compressive or tensile strain materials and both blue or red shifts in the bandgap can be achieved depending on the types of intermixing. The recent advancement in intermixing modified optical properties, such as absorption, refractive index as well as electro-optics effects are discussed. In addition, this paper will place a strong emphasis on the device application of the intermixing technology. The advantage of being able to tune the material provides a way to improve the performance of photodetectors and modulators. Attractive distributed-feedback and vertical cavity laser dynamics have been shown due to some unique device physics of the quantum well intermixing. Several state-of-the-art results will be summarized with an emphasis on its future development and directions.

Key words: Quantum Well Intermixing, Thermal Interdiffusion, Optical Properties of Quantum Well, Optical Devices, Optoelectronic Devices.

1. INTRODUCTION

A practical technique for integrating active and passive photonic devices will produce an immense impact on information processing, distribution, and manipulation. It is expected to be as significant a technological advance as was the development of the electronic IC. However, despite substantial efforts made by a large number of groups worldwide over the last few years, and the increasing demand for multiwavelength optical networks generated by the exponential growth of the internet and the World Wide Web in particular, this utopian vision has yet to be realized, where a consequence of the magnitude of the technological challenges is involved. For practical photonic IC's, practicality mandates low manufacturing cost and high reliability (low operating cost) even at the expense of somewhat reduced performance. With this in mind, we can establish the most important requirement for monolithically integrating optoelectronic devices of differing functionality's in order to achieve practical waveguiding photonic IC's. One of the primary requirements for this waveguiding is bandgap (operation wavelength) compatibility among the various optoelectronic devices. Although a number of techniques exist, each has its advantages and disadvantages - none is a panacea.

This paper presents a simple technique of fabricating integrated optoelectronic devices using spatially selective modification of quantum well (QW) shape after standard growth which, in turn, modifies QW bandgap energy. This diffused quantum well (DFQW) is a non-square quantum well produced by interdiffusion of constituent atoms through the heterointerface (Fig. 1). In the literature, DFQW is also referred to as quantum well mixing or intermixing (QWI) and quantum well disordering (IID). It is based on the fact that a QW is an inherently metastable system due to the large concentration

† Permanent Address : University of Hong Kong, Department of Electrical and Electronic Engineering, Pokfulam Road, Hong Kong. Email : ehli@eee.hku.hk

Part of the SPIE Conference on Physics and Simulation of Optoelectronic Devices VI
San Jose, California • January 1998 SPIE Vol. 3283 • 0277-786X/98/$10.00

gradient of atomic species across the well/barrier interface. For example, in InGaAs/InGaAsP QWs, the phosphorous concentration changes from 43% to 0% in a distance of less than 1 nm. At temperature above 750°C significant diffusion of atomic species will occur resulting in an interdiffusion of the well and barrier alloys. This process causes an increase in the bandgap energy. It can also be greatly enhanced by the presence of impurities or defects or vacancies in the vicinity of the interfaces of the QW, allowing interdiffusion to occur at temperatures that are substantially lower than that normally required. All these techniques are spatially selective, permitting interdiffusion enhancement only in the regions requiring a large bandgap, leaving other regions unmodified.

This bandgap modification is a powerful technique for monolithically integrating optoelectronic devices of varying functionalities on a single wafer. It is simple, has no deleterious effects on the optical, electrical, or lifetime properties of optoelectronic devices and, in fact, possesses surprising advantages (reducing polarization sensitivity and enhancing reflectance change). Since the process is easy to implement, it will simplify the fabrication of many complex photonic IC's and may finally render them practical enough to be adopted by industry. The advantage this technology is, through interdiffusion (intermixing), to accruate modify the QW materials (AlGaAs/GaAs, InGaAs/GaAs and InGaAs(P)/InP) bandgap and optical properties, and to make use of these tuning ability to integrate several device structures (such as waveguide-detector, laser-modulator, and laser-laser) to form photonic IC's. In particular, this allows a multi-section integrated structure will be fabricated for wide band-width and multi-wavelengths applications, such as to demonstrate its use for wavelength division multiplexing (WDM) in high bit rate communication systems.

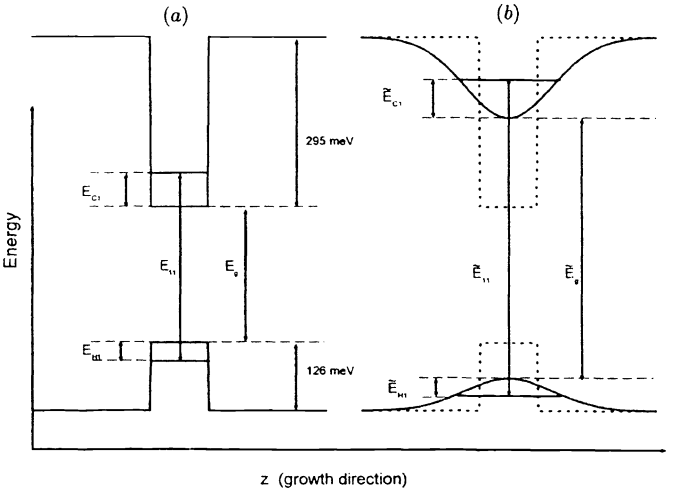

Figure 1. The conduction band and valence band potential energy profiles for an as-grown rectangular SQW structure and that of its interdiffused structure where $L_d \approx \frac{1}{2}L_z$. The tilde denotes the respective parameter in an interdiffused SQW and E_{cf} is the sum of the electron E_{c1} and hole E_{h1} confinement energies [24].

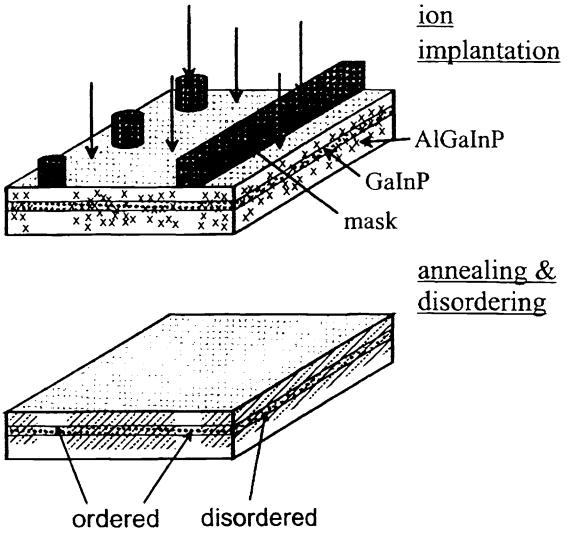

Figure 2. Scheme of selective disordering of a $CuPt_B$-ordered GaInP/AlGaInP heterostructure. Local implantation is achieved using implantation masks. After removing the masks and annealing the sample the implanted regions are disordered [3].

In recent years, great effort has been put in using DFQW as a tool. Last year, several remarkable papers have been published on advancing the intermixing process and technique [1-13, 60]. The interdiffusion mechanism and determination of the diffusion rate as well as their understanding are also being studied [14-21]. Bandgap engineering on the band structure and confinement states continuous to be developed [22-17]. There are extensive work on the modified optical properties as a result of intermixing [28-39] as well as on its application to advancing the device performance [40-52]. In addition, report of reviews have been made on IID by Holonyak in 1988 [53], on the process of DFQW optoelectronics by Weiss in 1990 [54], and on QWI by Marsh in 1993 [55]. More recently reviews have been published by Cohen [56] on diffusion and point defects and by

Li [57] on material and device advances. There are also one reprint series [58] and another monograph [59] on this subject to be published very soon.

In this paper, we aim to make a summary on some of the latest progress and development in DFQWs with particular attention pay to materials and device physics.

2. TECHNIQUES FOR MODIFYING INTERDIFFUSION RATES IN QWs

2.1 Ion Implantation

Ion Implantation is a technique in which direct injection of ionized, energetic atoms or molecules into a solid is employed. The ions injected will carry energies ranging from a few keV to several MeV, and implant doses from 10^{10} to more than 10^{16} ions/cm^2. Using small implantation energy, the damage introduced to the lattice structure will be reduced but with a decrease in the penetration depth, while with small dose of implants, there will be lesser enhancement of diffusion rate.

Ion Implantation will significantly enhance the interdiffusion rate, and control the lateral and vertical depth of diffusion precisely. Different combinations of ions and substrates are possible and the most commonly used ones are p-type ions (Zn, Be), n-type ions (Si), neutral type ions (O), and constituent ions (Al, Ga, As) in AlGaAs/GaAs. It was reported that the use of neutral ions (including constituent ions) can prevent the production of free carriers induced by the charged ions (n-type or p-type) which will introduce propagation loss and thus reduce the refractive index of the intermixed QW materials. Recent application of different implants are discussed as follows.

F implantation induced Ga/InGaP QW disordering has been performed in conventional furnace and in lamp annealing enviroment [6]. Group-V intermixing is found to be substantially enhanced for certain implantation and annealing conditions. There is another study on the spatial resolution achieved by implantation that is fine enough to produce distributed-feedback (DFB) structures for lasers [3]. Lateral order/disorder structures were achieved by masked implantation (Fig. 2) using high resolution electron beam lithography for the definition of wire and dot implantation masks down to 35 nm width.

The diffusion and QWI effects of the neutral impurities fluorine and boron in p- and n-type AlGaAs in the GaAs/AlGaAs system have been reported [25]. Boron was found to show significant diffusion in p-doped AlGaAs material but only exhibited a very small amount of diffusion in n-doped material after furnace annealing. Boron was also found to retard intermixing in p-AlGaAs. The mechanism of boron IID in n-AlGaAs was proposed to be attributed to both the diffusion of point defects generated during ion implantation. Results from fluorine IID suggest the possibility of the ionization of fluorine which gives rise to a higher electron concentration during annealing, leading to higher degrees of intermixing in n-AlGaAs.

2.2 Rapid Thermal Annealing (RTA)

RTA is an essential step in impurity diffusion. Since impurity diffusion process undergoes a very slow rate on its own at conventional conditions, RTA is therefore used to promote its diffusion rate. RTA under temperature ranging from 900 to 1125 ^{0}C leads to substantial increase in interdiffusion rate. Most of the annealing is usually performed in the range from 400 to 1000 ^{0}C, and under a chemical environment with N_2 or even in vacuum to prevent oxidation to occur.

The influence of RTA on the performance characteristic of GaInP/AlGaInP QW lasers which were grown by all-solid-source molecular-beam-epitaxy has been studied [8]. It was found that when the laser structure were annealed the threshold current density of the lasers decrease significantly. Another study on the influence of growth conditions on Al-Ga interdiffusion in low-temperature grown AlGaAs/GaAs MQW were characterized by photoluminescence (PL) spectroscopy [7]. The enhancement of interdiffusion was found to be strongly dependent on the growth and annealing conditions.

2.3 Impurity Free Vacancy Diffusion (IFVD)

The mechanism of IFVD requires the encapsulation of MQW samples by a dielectric cap such as SiO_2 or Si_3N_4 and then annealing at high temperature around 850 ^{0}C ~ 900 ^{0}C for 30 to 200 seconds. This will lead to out-diffusion of Ga into the cap and vacancies are generated on the group III sublattice that diffuse to the barriers and promote the interdiffusion in the MQWs. By using different combination of caps, selective area bandgap control is possible.

A phosphorus-doped silica (SiO_2:P) cap containing 5 wt% P has been demonstrated to inhibit the bandgap shifts of p-i-n and n-i-p GaAs/AlGaAs QW laser [5]. Bandgap shift differences as large as 100 meV have been observed from samples capped with SiO_2 and SiO_2:P . A report on the stress dependence in SiO_2 / Si_3N_4 encapsulation-based layer disordering of GaAs/AlGaAs QW has been published [10]. Comparative study reveals opposite behaviors for patterned Si_3N_4 covered with SiO_2 and patterned vice verses. In the former, layered disordering occurs under the Si_3N_4 strips and in the latter, layer disordering suprisingly occurs under the Si_3N_4 strips while it is inhibited in the SiO_2 capped areas. These results are in agreedment with a proposed interdiffusion model based on the effect on Ga vacancies, which are responsible for the layer disordering.

The advantage of using IFVD is that it is a simple method which requires much less equipment to perform. IFVD can create large bandgap energy shifts without these disadvantages of IID. However, using IFVD will increase the number of etching steps needed to control the thickness of SiO_2. Moreover, control of oxygen composition in SiO_xN_y is complex.

2.4 Laser Assisted Disordering (LAD)

Laser induced QW intermixing has been studied for some time, It is a direct write process that can pattern impurity induced layer disordering. This technique employs a highly focused Ar^+ laser beam. For fabrication of AlGaAs-GaAs DFQW, the laser beam with lasing wavelength of 488 nm, is scanned through the heterostructure sample which is encapsulated with a 90 nm layer of Si-Si_3N_4. Its scan speed can be as high as 85 μm/s. The laser beam interaction region will result in a smooth cylindrical section on the micron scale. Annealing is then applied to drive the Si into the as-grown crystal, resulting in a local mixing of the crystal layers. Alternatively, pulsed photoabsorption-induced disordering (PAID) technique can be used to selectively intermix GaInAs/GaInAsP QW structure, which has been studied by the use of high spatial resolution time-resolved PL. Measurements showed that a reduction in the non-radioactive recombination time of nearly two orders of magnitude as a result of this intermixing technique.

However the LAD can required high power densities to melt the material and can thus cause an undesirable redistribution of dopants out with the active region of the device. The spatial selectivity of PAID is also limited by lateral heat flow. For monolithic integration of optical devices, this leads to poor performance as the interface abruptness is ~ 100 μm. A variation of the PAID technique, which has a better spatial resolution has been developed using a pulsed laser irradiation [9]. It involves irradiating the InP-based QW material with high-energy Q-switched Nd:YAG laser pulses. Absorption of the high energy pulses results in bond breaking and disruption to the lattice, leading to a localized increase in the density of point defects. Measurements of the spatial resolution of this pulsed PAID technique show it to be better than 20 μm.

The laser assisted technique is a flexible process for optoelectronic device and circuit fabrication. However, a direct-write system is not an optimum configuration for many application. For example, commercial production of diode lasers is based upon high yield, high throughput techniques such as photolighography. Further improvement is required.

3. DIFFUSION MECHANISM

An atomic-scale model for the kinetics of intermixing of GaAs/AlGaAs quantum confined heterostructure has been proposed [15]. The model starts from first principles and views the vacancy diffusion length as a random walk which is

characterized by hop (Fig. 3) with rates determined through diffusion coefficients. Agreedment within 30% of the measurements was obtained for values of the surface release velocity > 1 μm/s.

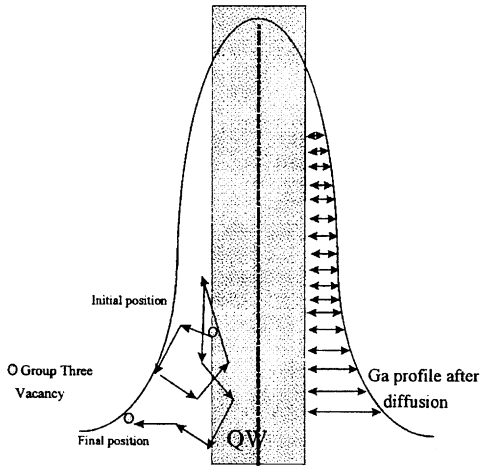

Figure 3. Schematic diagram of the lattice hops comprised in Ga outdiffusion from the quantum wells, illustrating the random walks associated with the group three vacancy diffusion [15].

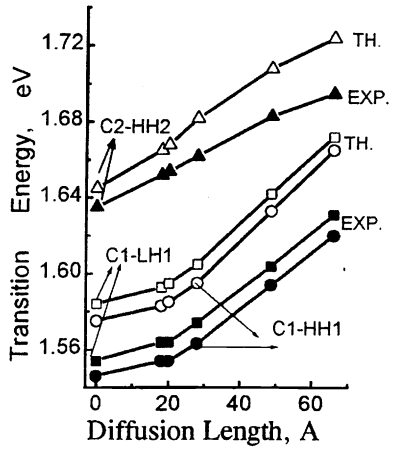

Figure 4. Transition energies (in eV) for diffused quantum wells, as a function of the diffused length L_D (in Å). The value if L_D = 0Å corresponds to the well width of 100Å (35 monolayers) of the initial as-grown rectangular quantum well: theory (th.) and experiment (exp.); transitions (C1-HH1), (C1-LH1), and (C2-HH2) [26].

The effects of thermally induced compositional disordering on the luminescence from two-dimensional and zero-dimensional high In (50%) InGaAs/GaAs QW are examined [18]. Quantum mechanical numerical calculations have been used to obtain values for diffusivities. Activation energies for interdiffusion (3.5 ± 0.3eV) are found to be similar to low In QWs. Transient behavior has been shown in the initial stage of interdiffusion. Another study has been conducted to use interdiffusion induced vacancy, as aprobe, to simultaneously measure the interdiffusion coefficient [17]. The measured vacancy concentration is about 2×10^{17} cm^{-3}. This result shows that the vacancy concentrations in GaAs are not at thermal equilibrium concentrations as has been widely assumed. The activation energy found for the intermixing is InGaAs/GaAs is known to be governed solely by the activation term for vacancy diffusion which is calculated to have an activation energy of 3.4 ± 0.3 eV.

The interdiffusion coefficients of the cations and anions in InGaAs/InP superlattices have been determined with and without SiO_2:P capping layers [19]. Double crystal X-ray diffraction and low temperature PL measurements are used. Simulation with the proper selection of the interdiffusion coefficients for fitting the interface strain profile and PL transition energies are used to obtained diffusion coefficients of 5.8×10^{-17} cm^2/s (anion) 2.9×10^{-17} cm^2/s (cation). The effect of strain and temperature on anomalously large interdiffusion in InAsP/InP heterostructures [20]. Evidence has been found for large, strain dependent interdiffusion and for the existence of a "critical strain" in a set of InGaP layers grown on InP substracts : if the strain is about 2% or more, much P-As mixing between the layer and substract occurs, but for smaller strain the mixing is greatly decreased.

Group-V sublattice interdiffusion in GaAsP/GaAs and GaAsSb/GaAs superlattices under various arsenic vapor pressures has been studied [14]. The diffusion coefficient was measured by secondary ion mass spectroscopy and cathodoluminscence spectroscopy. The interdiffusion coefficient was higher under arsenic-rich conditions than under gallium-rich conditions, pointing to an interstitial-substitutional type of diffusion mechanism.

4. BAND ENGINEEERING

Calculation has been preformed on the energy values and the spatial distributions of the bound electronic states in some diffused quantum wells [26]. The calculations are performed within the virtual crystal approximation, sp^3s^* spin dependent empirical tight-binding model and the surface Green function matching method. Good agreement is found to match experimental data (Fig. 4). For diffusion lengths less than 20 Å the optical transition between the ground electron and hole states is less sensitive to the diffusion length changes than the transitions between the excited electron and hole states. Another study on the behavior of the subband structure of AlGaAs/GaAs single quantum well structures due to interdiffusion shows that the variations of the allowed interband transitions with interdiffusion are determined by confinement and compositional energy changes in the quantum well [24]. The understanding of these is interrelated, and they are strong functions of the as-grown well width. In particular, results demonstrate that the higher-order transitions are more sensitive to interdiffusion than the ground state transitions during the early stages of interdiffusion.

Band gap modification in Ne^+-ion implanted InGaAs/InP (for various Ga concentrations) and InAsP/InP (for 32% As) quantum well structures has been studied by low temperature PL spectra [27]. The maximum usable high temperature anneal for inducing the intermixing using an InP proximity cap is found to be ~700 degrees C for 13 s. A second low-temperature (300 degrees C) anneal, following the high-temperature (700 degrees C) anneal, is found to induce greater band gap changes than the simple one-step anneal at 700 degrees C. The changes are found to be approximately proportional to the difference of bandgap energy between the well and the barrier materials; the proportionality coefficient increases with ion dose and reaches a maximum at a dose of $\sim 2 \times 10^{13}$ cm^{-2}. Another study on the effects of defect-enhanced, impurity-free, quantum-well(QW)-barrier compositional intermixing caused by the SiO^2 cap annealing at 750 degrees C of a 1.5-μm InGaAsP/InP MQW laser structure have been studied by PL [22]. A substantial band-gap blue shift, as much as 112 nm (~66 meV), was found in the structure and the value of the shift can be controlled by the anneal time. The amount of the shift does not depend on the thickness of the SiO^2 cap layer. The lasing wavelength of the laser produced with the SiO^2 cap has a 78 nm blue shift over that of the laser without the cap.

Wavefunction engineering has also been explored [23]. QW potentials are engineered to control the energy level shifts and wavefunction localization induced by semiconductor alloy intermixing. A few monolayers of a semiconductor with a different band gap can be inserted at the node or at the crest of wavefunctions with different parities to enhance the interdiffusion-induced interband transition energy-shifts, or to manipulate the intersubband transition energies.

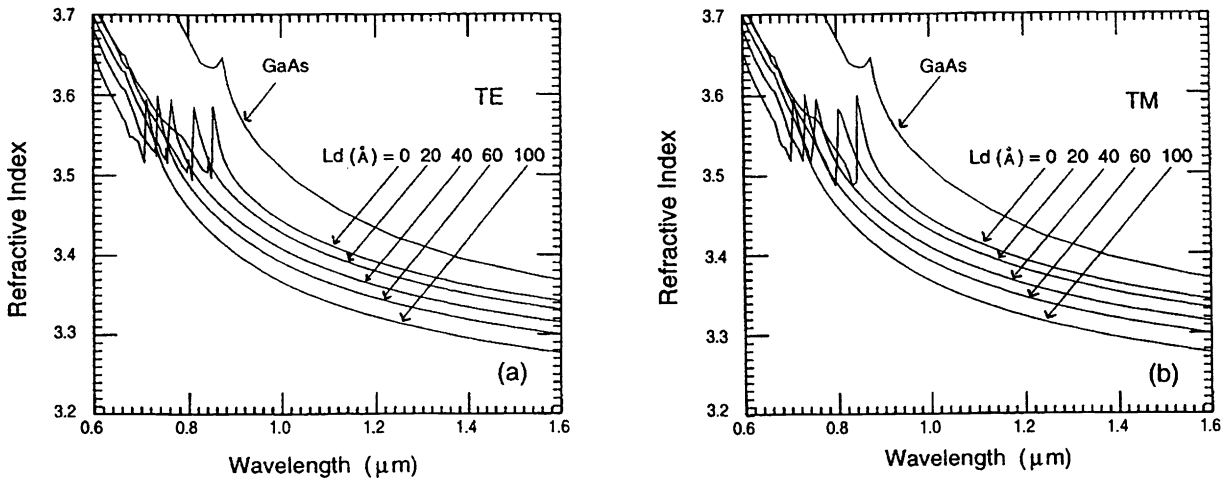

Figure 5. The refractive index spectra of $Al_{0.3}Ga_{0.7}As$/GaAs QW with L_z = 100Å; for L_d = 0, 20, 40, 60, 100Å. (a) TE polarization. (b) TM polarization [35].

5. OPTICAL PROPERTIES

5.1 Refractive Index

A model has been developed for the polarization dependent refractive index (Fig. 5) of interdiffused AlGaAs/GaAs QW at room temperature for wavelengths ranging from 0.6 to 2 μm [35]. The present model is based on a semianalytic and semiempirical method through the Kramers-Kronig transformation. The multi-QW structures, including the exciton effect and above barrier gap contributions, are fully considered in this model. The distinct structures at energies of the E_0, $E_0+\Delta_0$, E_1 and E_2 critical points are revealed. Moreover, the birefringence at room temperature is also analyzed in the wavelength range varying from 0.7 to 1.0 μm. The calculated refractive index results are in satisfactory agreement with the experimental measurements over the QW band edge, i.e., 0.8-0.9 μm. The effect of interdiffusion on the change of refractive index is discussed. The polarization dependent absorption coefficients are also calculated with all the bound excitons (Fig. 6), and results agree well with experiments. These results are important, since refraction index in a particular wavelength region of interest, where experimental data are not available, can be determined and thus are very useful in the design of devices.

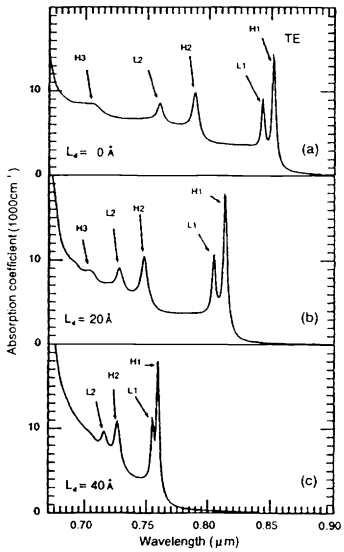

Figure 6. Absorption coefficient TE spectra as a function of photon energy. Heavy and light hole excitonic transitions are indicated by H and L. (a) L_d = 0Å, (b) L_d = 20Å, (c) L_d = 40Å [35].

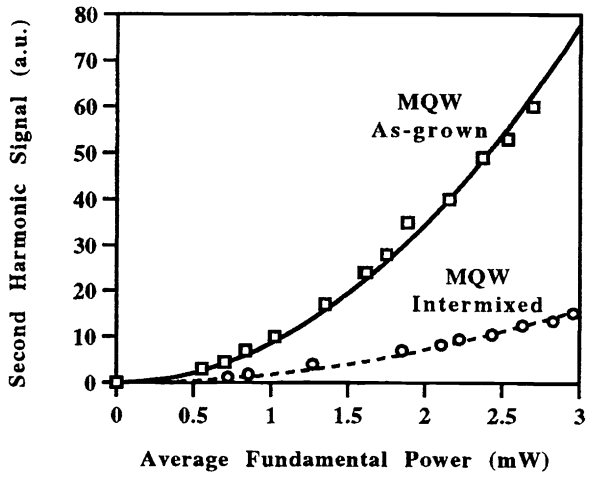

Figure 7. Unphase-matched TM-polarized second harmonic intensities from ACQW waveguides fabricated from as-grown and intermixed material for a 1.52μm TM-polarized fundamental input. The symbols correspond to data points and the curves are square law best fits [38].

5.2 Electro-absorption and Electro-Optics

The effects of Group III and Group V interdiffusions with a varied as-grown well width and P concentration in the quaternary InGaAsP quantum well material have been theoretically studied [34]. Interesting features of multiple mini-well profiles, generated by interdiffusion induced compressive and tensile strains, have been obtained and varying envelope overlapping of the electron-hole wave functions has been observed. The results show that the interdiffusion of the Group III elements with a well width of 10 nm offers a wide adjustability of the operation wavelength, enhances Stark shift, and reduces absorption loss, although they bear the shortcomings of low electro-absorption and contrast ratio. Several methods are proposed here to recover the contrast ratio with a maximum improvement of 66%. For the Group V interdiffusion of a 10-nm-wide as-grown well, a low absorption loss and a large Stark shift will result, while that of a narrowed well can widen the band-edge

wavelength adjustability with a large electro-absorption. These results are important for the development of electro-absorptive InGaAsP/InP diffused QW modulators.

The demonstrate the use of interdiffusion in the realization of polarization insensitivity at the band-edge has been studied theoretically [31]. Two InGaAs-InP QW as-grown structures have been investigated: one with lattice-matched condition and the other with small as-grown tensile strain (0.15%). The interdiffusion is considered to take place on the Group V (As and P) sublattice only. As a result, a tensile strain is produced which merges the heavy- and light-hole states in order to achieve polarization insensitivity. Criteria to develop polarization-insensitive QW's using interdiffusion are presented here. When the two-phase interdiffusion mechanism is modeled, the results show that the well barrier interfaces of the QW maintain an abrupt profile while the well width remains constant after interdiffusion. The two interdiffused QW structures considered here can produce polarization insensitive electroabsorption at operation wavelengths around 1.55 μm. The one with lattice-matched condition is particularly attractive since it only requires an easy (high-yield) fabrication process with a simple postprocessing thermal annealing to achieve polarization insensitivity.

5.3 Optical Gain

A theoretical analysis on the effect of interdiffusion on the optical gain, differential gain, linewidth enhancement factor, and the injection current density of InGaAs/GaAs and AlGaAs/GaAs QW lasers has been reported [29]. The electron and hole subband structure has been calculated including the effects of valence band mixing and strains. The optical results show that the gain spectrum can be blue-shifted without an enormous increase in the injection current density. Imposing an upper limit (416 $A \bullet cm^{-2}$) on the injection current density of a typical laser structure, it has found that the InGaAs/GaAs and AlGaAs/GaAs QW lasers can be blue-shifted by 24 and 54 nm, respectively. These predictions compare well with the tuning ranges of 53 and 66 meV found for AlGaAs/GaAs QW's in some experiments. This indicates that the interdiffusion technique is useful for the tuning of laser operation wavelength for multiwavelength applications.

5.4 Nonlinear Optical Effects

Linear and third-order conduction intersubband absorption coefficients have been analyzed in interdiffused lattice matched AlGaAs/GaAs and strained InGaAs/GaAs QW structures [33]. The variation of diffusion lengths has imposed a vast change in subband states energies and causes the transition energies between the lowest two subbands to shift in both red and blue depending on the QW structure. This modification provides a wide range of operation wavelengths (5 to 26 μm) in the mid to far IR region. In order to perform a comprehensive analysis, interdiffused quantum wells with different Al or In concentration, well width and optical field intensity are analyzed. The extent of the range of absorption coefficient due to interdiffusion in these QWs are then examined. Potential devices applications such as photodetectors and modulators operating in this IR regime are proposed by using the interdiffused QW materials.

A demonstration of the QW intermixing technique has been put on the control of second-order nonlinearity $\chi_{zzz}^{(2)}$ in an AlGaAs asymmetric coupled QW waveguide structure at 1.52 μm [38]. PL measurements also indicate that the spatial resolution of the impurity-free vacancy disordering process used for QWI is better than 1.5 μm which should be sufficient for first-order quasiphase-matched second harmonic generation. Fig. 7 shows the up-conversion efficiency has been reduced by a factor of ~ 4.8 as a result of the intermixing process. Further experimental evidence has been shown to demonstrate the feasibility of a promising new quasi-phase-matching technique in AlGaAs multiple-quantum-well waveguides (Fig. 8) [39]. Non-phase-matched second-harmonic-generation measurements indicate that, for sub-half-bandgap excitation near 1.5 μm, QW intermixing by impurity-free vacancy disordering results in a reduction of the nonlinear susceptibility $\chi_{zxy}^{(2)}$ (~340 pm/V) by 17%. Relatively low intermixed waveguide losses, and the high spatial resolution of the impurity-free vacancy disordering process, suggest that periodic intermixing along the direction of propagation should lead to useful frequency-conversion efficiencies.

6. DEVICES

6.1 Lasers

The effects of defect-enhanced, impurity-free, QW-barrier compositional intermixing caused by the SiO2 cap annealing at 750 °C of a 1.5-m InGaAsP/InP multiple quantum-well (MQW) laser structure have been studied by PL [41]. A substantial band-gap blue shift, as much as 112 nm (~ 66 meV), was found in the structure and the value of the shift can be controlled by the anneal time. The amount of the shift does not depend on the thickness of the SiO_2 cap layer. Ridge-waveguide lasers were fabricated on the different areas of the wafer, with and without a SiO_2 cap during a 60 s anneal. The lasing wavelength of the laser produced with the SiO_2 cap has a 78 nm blue shift over that of the laser without the SiO_2 cap.

By using phosphorous doped (5% wt P) silica as masking material and standard silica capping to promote QW interdiffusion, GaAs-AlGaAs ridge lasers with integrated transparent waveguides were fabricated [44]. With a selective differential blue-shift of 30 nm in the absorption edge, devices with 400-μm/2.73-mm-long active/passive sections exhibited threshold currents of 8 mA in CW operation, only 1 mA higher than that for normal lasers of the same active length and from the same chip. This 14% increase in threshold current was accompanied by a slope efficiency decrease of 40%. Losses of 3.2 cm^{-1} were measured in the passive waveguides at the lasing wavelength using the Fabry-Perot resonance method. This value is among the lowest reported so far using an impurity-free disordering technique.

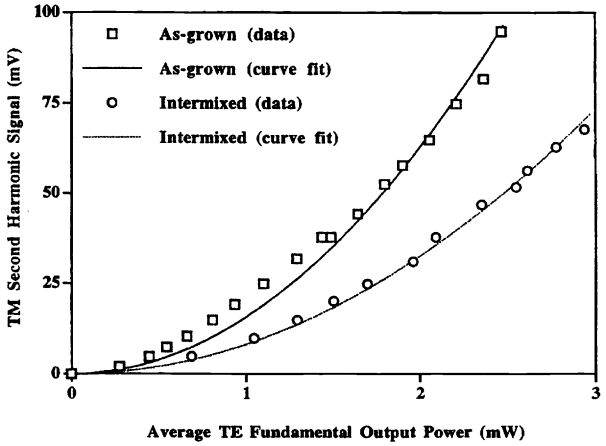

Figure 8. TM-polarized second-harmonic signal as a function of the TE-polarized fundamental output power for as-grown and intermixed AlGaAs MQW ridge waveguide devices with sub-half-bandgap excitation at 1.524μm [39].

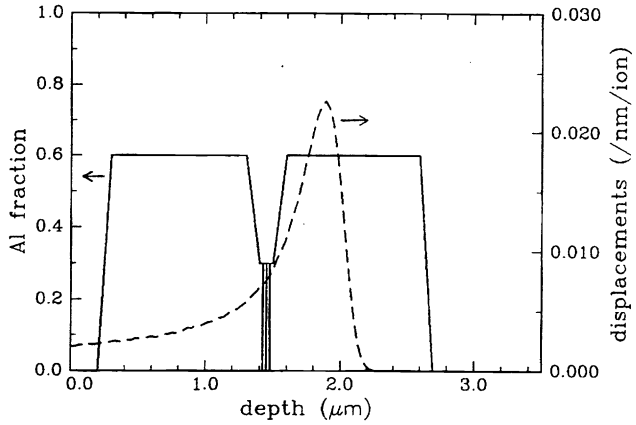

Figure 9. Schematic of the GRINSCH quantum well laser structure used in this study. Also shown is the calculated displacement profile for 240 keV protons [51].

Reflectance modulation measurements have been used to determine facet temperatures of InGaAs/GaAs double-QW graded-index separate-confinement heterostructure ridge-waveguide lasers possessing band gap tuned passive cavity sections [48]. It is found that the incorporation of transparent extended cavities, produced by ion-implantation enhanced QW intermixing, significantly decreases the laser facet temperatures. The reduced photoabsorption occurring at the facets, achieved by the QW intermixing process, should lead to increases in both the maximum optical power levels and device longevity prior to the onset of catastrophic failure.

Proton irradiation followed by rapid thermal annealing was used to selectively induce layer intermixing and thus shift the emission wavelengths of GaAsAlGaAs graded-index separate-confinement-heterostructure QW lasers (Fig. 9) [51]. Up to 40 nm shifts were observed in 4 μm ridge waveguide devices irradiated to a dose of 1.5×10^{16} cm^{-2}. Although the wavelength shifts were accompanied by some degradation in the lasing threshold current and differential quantum efficiency, they were still

quite acceptable at moderate wavelength shifts. This technique provides a simple and promising postgrowth process of integrating lasers of different wavelengths for wavelength-division-multiplexing applications.

A two-dimensional self-consistent physical modeling has been employed to a particularly promising lateral current injection laser in order to gain insight into the physical mechanisms governing the operation of this family of devices [49]. Substantial benefits have been demonstrated from improved hole injection facilitated by relatively light p-type doping of barrier layers; from lateral shifting of the transverse junction to improve the overlap between the photon field and material gain; and from creating a lateral heterobarrier via QW intermixing in order to confine carriers in the lateral direction. It is found that with a number of relatively minor physically motivated modifications to existing fabrication processes, lateral injection lasers have the potential to exhibit greatly improved performance characteristics and to realize thereby their tremendous potential as enablers of optoelectronic integrated circuits and novel device structures.

DFB and Fabry-Perot (FP) semiconductor lasers with step (Fig. 10) and periodic interdiffusion quantum-well structures have been proposed for high-power single-longitudinal-mode operation [52]. It is shown that the phase-adjustment region formed by the diffusion step (i.e., step change in optical gain and refractive index) counteracts the influence of spatial hole burning, especially for DFB lasers with large coupling-length products biased at high injection current. Furthermore, it is found that with careful design of the diffusion grating (i.e., grating period and amount of diffusion extent) of FP lasers, side-mode suppression ratio can be enhanced and threshold current density can be minimized to a satisfied level.

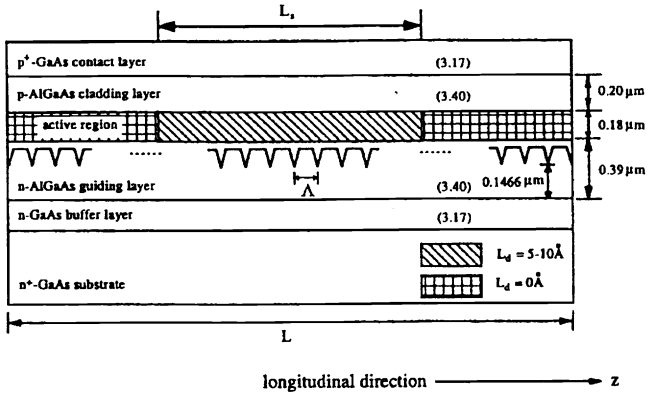

Figure 10. Schematic of the DFB laser with diffusion step profile. L_s is the length of the diffusion step and L_d is the diffusion length [52]

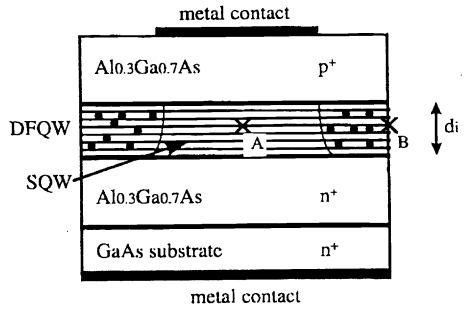

Figure 11. The cross section of the waveguide-type phase modulator, where the guiding region contains square QW's after interdiffusion [43].

6.2 Optical modulator and Detector

A Fabry-Perot reflection-type modulator which uses interdiffused AlGaAs-GaAs QW as the active cavity material has been studied and optimized theoretically [42]. An asymmetric Bragg reflector structure (modeled by transfer matrices), with a doped depletion layer in the heterostructure, has been considered. Results show improvement in modulation property over its as-grown rectangular QW modulator. In particular, the change of reflectance in the diffused QW modulator is almost 0.6 to 0.7, which is higher than that of the typically available values (~0.5 to 0.6), while the OFF-state on-resonance reflectance is almost close to zero. The operation voltage is also reduced by more than half as the interdiffusion becomes extensive. The finesse of the more extensively diffused quantum well also increases. Both of these features contribute to an improvement of the change of reflectance in the modulator. The operation wavelengths can be adjusted over a range of 100 nm. However, the absorption coefficient change of the diffused quantum well increases only when there is a small amount of interdiffusion.

Waveguide phase modulators (Fig. 11), with 0.5- and 1-μm QW active regions which are defined by impurity-induced disordering are investigated theoretically [43]. By controlling the extent of the interdiffusion in the lateral claddings, the

refractive index difference between the core and claddings is used to provide single-mode operation. Strong optical confinement, which is required to produce single-mode high-efficiency modulation, requires the peak impurity concentration to be at the center of the QW active region. Moreover, the annealing time needs to be optimized so that single mode can be maintained at the desired bias field. A low dopant concentration is also expected to minimize the destruction of the modulator structure. The results show that since the core/cladding interface is graded, the width of the metal contact is important. A comparison of modulation efficiency for active layer thicknesses of 0.5 and 1.0 μm shows that the 0.5-μm one is a more efficient structure and its absorption loss can be reduced by increasing the applied field from 50 to 100 kV/cm.

The effect of RTA on important detector characteristics such as dark current, absolute response, noise, and detectivity is investigated for QW infrared photodetectors (QWIP) operating in the 8-12 μm wavelength regime [50]. A comprehensive set of experiments is conducted on QWIPs fabricated from both as-grown and annealed multiple-QW structures. RTA is done at an anneal temperature of 850 degrees C for 30 s using an SiO_2 encapsulant. In general, a decrease in performance is observed for RTA QWIP when compared to the as- grown detectors. The peak absolute response of the annealed QWIPs is lower by almost a factor of four, which results in a factor of four decrease in quantum efficiency. In addition, a degraded noise performance results in a detectivity which is five times lower than that of QWIPs using as grown structures. Theoretical calculations of the absorption coefficient spectrum are in excellent agreement with the experimental data.

6.3 Integrated Photonic Devices

The bandgap of InGaAs-InGaAsP MQW material can be accurately tuned by photoabsorption-induced disordering (PAID), using a Nd:YAG laser, to allow lasers, modulators, and passive waveguides to be fabricated from a standard MQW structure [45]. The process relies on optical absorption in the active region of the MQW to produce sufficient heat to cause interdiffusion between the wells and barriers. Bandgap shifts larger than 100 meV are obtainable using laser power densities of around 5 W mm^{-2} and periods of illumination of a few minutes to tens of minutes. This process provides an effective way of altering the emission wavelengths of lasers fabricated from a single epitaxial wafer. Blue shifts of up to 160 nm in the lasing spectra of both broad-area and ridge waveguide lasers have been achieved (Fig. 12). The bandgap-tuned lasers are assessed in terms of threshold current density, internal quantum efficiency, and internal losses. The ON/OFF ratios of bandgap-tuned electroabsorption modulators were tested over a range of wavelengths, with modulation depths of 20 dB obtained from material which has been bandgap-shifted by 120 nm, while samples shifted by 80 nm gave modulation depths as high as 27 dB. Single-mode waveguide losses are as low as 5 dB cm^{-1} at 1550 nm. Selective-area disordering has been used in the fabrication of extended cavity lasers. The retention of good electrical and optical properties in intermixed material demonstrates that PAID is a promising technique for the integration of devices to produce photonic integrated circuits.

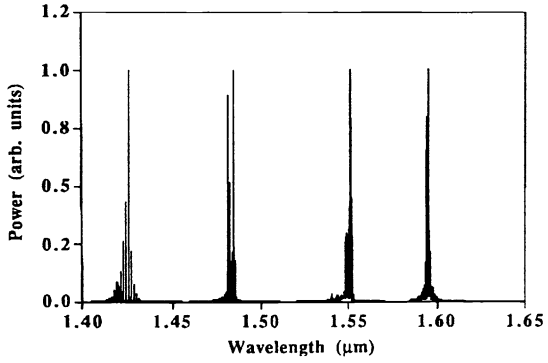

Figure 12. Emission spectra of bandgap-tuned oxide stripe lasers [45].

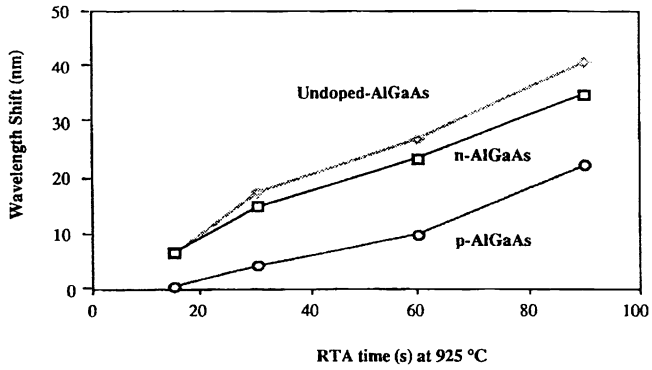

Figure 13. Wavelength shifts as a function of annealing time obtained from SiO_2 capped intrinsic, n-I-o, and p-I-n samples annealed at 925°C [46].

By using the technique of QWI, monolithically integrated passive, and active waveguides can be fabricated [40]. It has been shown that mode-locked extended cavity semiconductor lasers with integrated low-loss passive waveguides display superior performance to devices in which the entire waveguide is active: the threshold current is a factor of 3-5 lower, the pulsewidth is reduced from 10.2 ps in the all active laser to 3.5 ps in the extended cavity device and there is a decrease in the free-running jitter level from 15 to 6 ps (10 kHz-10 Mhz).

Impurity-free vacancy disordering using SiO_2 and SrF_2 dielectric caps (Fig. 13) to induce selective quantum-well (QW) intermixing in the GaAs-AlGaAs system is studied [46]. The intermixing rate of IFVD was found to be higher in n-i-p and intrinsic than in p-i-n structures, which suggests that the diffusion of the Group III vacancy is not supported in p-type material. Single-mode waveguides have been fabricated from both as-grown and bandgap-tuned double-quantum-well (DQW) laser samples. Propagation losses as low as 8.5 dB cm^{-1} were measured from the bandgap-tuned waveguides at the lasing wavelength of the undisordered material, i.e., 860 nm. Simulation was also carried out to study the contribution of free-carrier absorption from the cladding layers, and the leakage loss induced by the heavily p-doped GaAs contact layer. It was found that the leakage loss contributed by the GaAs cap layer is significant and increases with wavelength. Based on IFVD, the fabrication of multiple-wavelength lasers and multichannel wavelength division multiplexers were also demonstrated using the one-step "selective intermixing in selected area" technique. This technique enables one to control the degree of intermixing across a wafer. Lasers with bandgaps tuned to five different positions have been fabricated on a single chip (Fig. 14). These lasers showed only small changes in transparency current, internal quantum efficiency, or internal propagation loss, which indicates that the quality of the material remains high after being intermixed. Four-channel wavelength demultiplexers based on a waveguide photodetector design have also been fabricated (Fig. 15). Photocurrent and spontaneous emission spectra from individual diodes showed that the absorption edge was shifted by different degrees due to the selective degree of QW intermixing. The results obtained also imply that the technique can be used in the fabrication of broad-wavelength emission superluminenscent diodes.

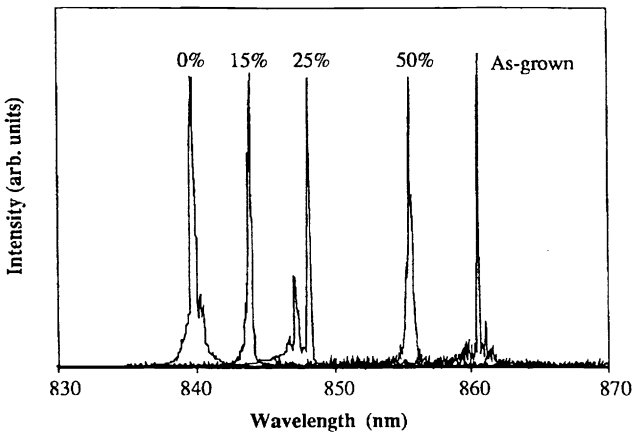

Figure 14. The lasing spectra of lasers bandgap-shifted using the SISA technique [46].

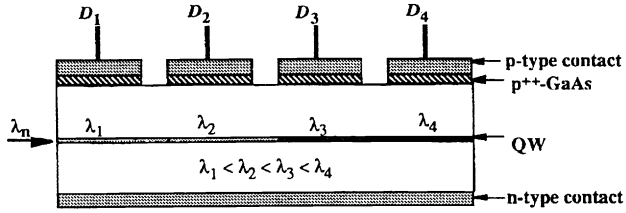

Figure 15. Schematic cross section of the four-channel demultiplexing wavefuide photodetector. The length of each diode is 300 m and the spacing between diodes is 100 m. Light was injected from the cleaved edge of diode D_1 during the photocurrent measurement [46].

7. CONCLUSION

It can bee seen that QWI has introduced a very promising future in optoelectronics. In fact, development has advanced not only in improving performance, reliability, and integration of existing optical components, but also for cultivating novel optical functions. A planar, compatible photonic IC in which a variety of different optical devices are composed of a common as-grown MQW structure, is proposed. This integration technique does not require a re-growth process, and it should prove useful for a variety of integrated devices, including mode-locked lasers and lasers integrated with optical modulators. At

present, development for device enhancement and progressions is underway. In addition, wavelength demultiplexing modulator is foreseen as a new area of development in the very near future. Another aspect which is of interest will be towards the longer wavelengths (Mid to Far IR) using materials such as InGaSb/GaSb as well as towards the shorter wavelengths (visible to UV range) using materials such as InGaN/GaN. These are now being developed and will expand the area of application by using QW intermixing.

8. ACKNOWLEDGEMENT

This work is supported in part by the Research Grant Council (RCG) earmarked grant of Hong Kong.

9. REFERENCE

[1] T. Baron F. Kany, K. Saminadayar, N. Magnea, and R. T. Cox, Appl. Phys. Lett. **70**, 2963 (1997).
[2] D. Behr, R. Niebuhr, J. Wagner, K.H. Bachem, and U. Kaufmann, Appl. Phys. Lett. **70**, 363 (1997).
[3] M. Burkard, A. Englert, C. Geng, A. Muhe, F. Scholz, H. Schweizer and F. Phillipp, J. Appl. Phys. **82**, 1042 (1997).
[4] W.C.H.Choy, P.J.Hughes, B.L.Weiss, E.H.Li, A.N.O and D.Pavlidis, Appl. Phys. Lett., 1998. (accepted for publication)
[5] P. Cusumano, B.S. Ooi, A.S. Helmy, S.G. Ayling, A.C. Bryce, J.H. Marsh, B. Voegele and M.U. Rose, J. Appl. Phys., **81**, 2445 (1997).
[6] U. Das, B. Pathangey, Z. Osman, and T.J. Anderson, Appl. Phys. Lett. **71**, 1700 (1997).
[7] W. Feng, F. Chen, W.Q. Cheng, Q. Huang, and J.M. Zhou, Appl. Phys. Lett. **71**, 1676 (1997).
[8] M. Jalonen, M. Toivonen, P. Savolainen, J. Kongas, and M. Pessa, Appl. Phys. Lett. **71**, 479 (1997).
[9] B.S. Ooi, C.J. Hamilton, K. Mcilvaney, A.C. Bryce, R.M. Delarue, J.H. Marsh, and J.S. Roberts, IEEE Photon. Technol. Lett. **9**, 587 (1997).
[10] A. Pepin, C. Vieu, M. Schneider, H. Launois, and Y. Nissim, J. Vacuum Sci. & Tenhnol. B **15**, 142 (1997).
[11] K. Rammohan, D.H. Rich, M.H. Macdougal, and P.D. Dapkus, Appl. Phys. Lett. **70**, 1599 (1997).
[12] D.K. Sengupta, T. Horton, W. Fang, A. Curtis, J. Li, S.L. Chuang, H. Chen, M. Feng, G.E. Stillman, A. Kar, J. Mazumder, L. Li, and H.C. Liu, Appl. Phys. Lett. **70**, 3573 (1997).
[13] S. Yuan, Y. Kim, C. Jagadish, P.T. Burke, M. Gal, J. Zou, D.Q. Cai, D.J.H. Cockayne, and R.M. Cohen, Appl. Phys. Lett. **70**, 1269 (1997).
[14] U. Egger, M. Schultz, and P. Werner, J. Appl. Phys. **81**, 6056 (1997).
[15] A. Saher Helmy, J. S. Aitchison, J. H. Marsh, Appl. Phys. Lett. **71**, 2998 (1997).
[16] Z.H. Jafri, and W.P. Gillin, J. Appl. Phys. **81**, 2179 (1997).
[17] O.M. Khreis, W.P. Gillin, and K.P. Homewood, Phys. Rev. B. **55**, 15813 (1997).
[18] R. Leon, D.R.M. Williams, J. Krueger, E.R. Weber, M.R. Melloch, Phys. Rev. B **56**, R4336 1997).
[19] S.W. Ryu, B.D. Choe, and W.G. Jeong, Appl. Phys. Lett. **71**, 1670 (1997).
[20] D.J. Tweet, H. Matsuhata, P. Fons, H. Oyanagi, H. Kamei, Appl. Phys. Lett. **70**, 3410 (1997).
[21] S.F.Wee, M. K. Chai, K. P. Homewood, and W. P. Gillin, J. Appl. Phys. **82**, 4842 (1997).
[22] N. Cao, B.B. Elenkrig, J.G. Simmons, D.A. Thompson, and N. Puetz, Appl. Phys. Lett. **70**, 3419 (1997).
[23] S.Fafard, J. Appl. Phys. **82**, 3857 (1997).
[24] P.J. Hughes, B.L. Weiss, and H.E. Jackson, Semicond. Sci. Technol. **12**, 808 (1997).
[25] B.S. Ooi, A.C. Bryce, J.H. Marsh, and J.S. Roberts, Semicond. Sci. Technol. **12**, 121 (1997).
[26] S. Vlaev, and D. A. Contreras-Solorio, J. Appl. Phys. **82**, 3853 (1997).
[27] J.Z. Wan, J.G. Simmons, and D.A. Thompson, J. Appl. Phys. **81**, 765 (1997).
[28] M.C.Y.Chan, E.H.Li, and K.S.Chan, Physica B, 1998. (accepted for publication)
[29] M.C.Y.Chan, Y.Chan, and E.H.Li, IEEE J. Quantum Electronics, 1998. (accepted for publication)
[30] K.S.Chan, E.H.Li and M.C.Y.Chan, IEEE J. Quantum Electron. **34**, 157 (1998).
[31] W.C.H.Choy, E.H.Li, and J.Micallef, IEEE J. Quantum Electron. **33**, 1316 (1997).
[32] W.C.H.Choy and E.H.Li, Applied Optics, 1998. (accepted for publication)
[33] E.H. Li, Jpn. J. Appl. Phys. **36**, 3418 (1997).

[34] E.H.Li and W.C.H.Choy, J. Appl. Phys. **82**, 3861 (1997).
[35] E.H.Li, J. Appl. Phys. **82**, 6251 (1997).
[36] J.Micallef, J.L.Borg, and E.H.Li, Opt. Quantum Electron. **29**, 423 (1997).
[37] I.Shtrichman, D. Gershoni, and R. Kalish, Phys. Rev. B **56**, 1509 (1997).
[38] M.W.Street, N.D. Whitbread, C.J. Hamilton, B. Vogele, C.R. Stanley, D.C. Hutchings, J.H. Marsh, J.S. Aitchison, G.T. Kennedy, and W. Sibbett, Appl. Phys. Lett. **70**, 2804 (1997).
[39] M. W. Street, N. D. Whitbread, D. C. Hutchings, J. M. Arnold, J. H. Marsh, J. S. Aitchison, G. T. Kennedy, and W. Sibbett, Opt. Lett. **22**, 1600 (1997).
[40] F.Camacho, E.A. Avrutin, P. Cusumano, A.S. Helmy, A.C. Bryce, and J.H. Marsh, IEEE Photon. Technol. Lett. **9**, 1208 (1997).
[41] N.Cao, B.B. Elenkrig, J.G. Simmons, D.A. Thompson, and N. Puetz, Appl. Phys. Lett. **70**, 3419 (1997).
[42] W.C.H.Choy and E.H.Li, IEEE J. Quantum Electron. **33**, 382 (1997).
[43] W.C.H.Choy, B.L.Weiss and E.H.Li, IEEE J. Quantum Electron. **34**, 84 (1998).
[44] P.Cusumano, J.H. Marsh, M.J. Rose, and J.S. Roberts, IEEE Photon. Techonol. Lett. **9**, 282 (1997).
[45] A.McKee, C.J.. Mclean, G. Lullo, A.C. Bryce, R.M. Delarue, J.H. Marsh, and C.C. Button, IEEE J. Quantum Electron. **33**, 45 (1997).
[46] B. S. Ooi, K. McIlvaney, M. W. Street, A. Saher Helmy, S. G. Ayling, A. C. Bryce, J. H. Marsh, and J. S. Roberts, IEEE J. Quantum Electron. **33**, 1784 (1997).
[47] B.S.Ooi, C.J. Hamilton, K. Mcilvaney, A.C. Bryce, R.M. Delarue, J.H. Marsh, and J.S. Roberts, IEEE Photon. Technol. Lett. **9**, 587 (1997).
[48] P.G.Piva, S. Fafard, M. Dion, M. Buchanan, S. Charbonneau, R.D. Goldberg, and I.V. Mitchell, Appl. Phys. Lett. **70**, 1662 (1997).
[49] E. H. Sargent, G. L. Tan, and J. M. Xu, IEEE JTSQE **3**, 507 (1997).
[50] D.K.Sengupta, W. Fang, J.I. Malin, A.P. Curtis, T. Horton, H.C. Kuo, D. Turnbull, C.H. Lin, J. Li, K.C. Hsieh, S.L. Chuang, I. Adesida, M. Feng, S.G. Bishop, G.E. Stillman, J.M. Gibson, H. Chen, J. Mazumder, and H.C. Liu, J. of Electronic Materials **26**, 43 (1997).
[51] H. H. Tan and C. Jagadish, Appl. Phys. Lett. **71**, 2680 (1997).
[52] S.F.Yu, C.W.Lo, and E.H.Li, IEEE J. Quantum Electron. **33**, 999 (1997).
[53] D.G.Deppe, and N. Holonyak, J. Appl. Phys. **64,** R93 (1988).
[54] B.L. Weiss, Ed., Special Issue, Opt. Quantum. Electron. **23,** S799 (1991).
[55] J.H. Marsh, Semicond. Sci. Technol. **8**, 1136 (1993).
[56] R.M.Cohen, Mat. Sci. Eng. Rev. (1997).
[57] E.H.Li, Mat. Res. Soc. Symp. Proc. **450**, 353 (1996).
[58] E.H.Li, editor, *Quantum well intermixing for photonics*, SPIE Milestone Series (SPIE) 1998.
[59] E.H.Li, editor, *Semiconductor quantum well intermixing – material properties and optoelectronics applications*, Gordon and Breach (Philadelphia, USA) 1998.
[60] P.J.Hughes, B.L. Weiss, S. Tlali, and H.E. Jackson, J. Vac. Sci. Technol. **B 15**, 845 (1997).